

# The Pierre Auger Observatory: Results on Ultra-High Energy Cosmic Rays

Johannes Bluemer

Karlsruhe Institute of Technology KIT\*  
Postfach 3640, D-76021 Karlsruhe, Germany

for the Pierre Auger Collaboration  
Observatorio Pierre Auger, Av. San Martin Norte 304, 5613 Malargue, Argentina

August 14, 2019

Proceedings of the International Workshop on Advances in Cosmic Ray Science, Waseda University, Shinjuku, Tokyo, Japan, March 2008; to be published in the Journal of the Physical Society of Japan (JPSJ) supplement.

## Abstract

The focus of this article is on recent results on ultra-high energy cosmic rays obtained with the Pierre Auger Observatory. The world's largest instrument of this type and its performance are described. The observations presented here include the energy spectrum, the primary particle composition, limits on the fluxes of photons and neutrinos and a discussion of the anisotropic distribution of the arrival directions of the most energetic particles. Finally, plans for the construction of a Northern Auger Observatory in Colorado, USA, are discussed.

KEYWORDS: ultra-high energy cosmic rays, Auger Observatory, GZK, AGN, air shower

## 1 Introduction

The Earth's atmosphere is exposed to a flux of energetic particles from space. Their energies extend from the MeV range to at least  $10^{20}$  eV. The non-thermal energy spectrum follows a power law  $dN/dE \propto E^{-\gamma}$ ; the spectral index  $\gamma$  has a value

around  $-3$ ; it varies in certain energy regions indicating interesting possible changes in the composition and in the acceleration and propagation processes.

Diffusive shock acceleration is thought to be the basic mechanism that gives energy to charged cosmic ray particles. The maximum attainable energy is proportional to the particles' charge and to the product of shock velocity, magnetic field and size of the acceleration region [6]. Supernova remnants are candidates for the acceleration of galactic cosmic rays up to energies of several  $10^{17}$  eV. Of particular interest is the study of cosmic particles at the highest energies observed so far. As cosmic rays of energy greater than  $10^{19}$  eV are not confined by typical galactic magnetic fields, it is natural to assume that those are produced by extra-galactic sources. The list of the very few viable candidate sources for such energies includes active galactic nuclei (AGN), radio lobes of FR II galaxies, and gamma-ray bursts (GRBs). However, the short energy loss lengths indicate that particles of energy above  $10^{20}$  eV should come from sources within a 100 Mpc sphere. Astrophysical sources within our Galaxy are disfavoured. For a recent review of astrophysical sources, see [7]).

More than 40 years ago Greisen, Zatsepin and Kuzmin realized that the interaction of protons with cosmic microwave background photons would result in significant energy losses. The energy spectrum would show a flux suppression above a threshold energy of about  $6 \times 10^{19}$  eV, the GZK effect

\*KIT is the cooperation of Universität Karlsruhe (TH) and Forschungszentrum Karlsruhe GmbH

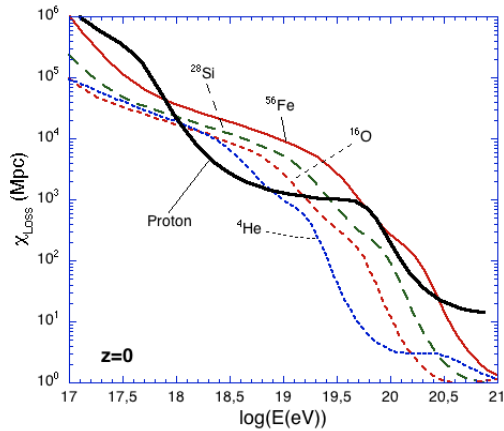


Figure 1: Energy loss lengths [5] of protons and nuclei calculated for a redshift  $z = 0$ . Iron nuclei have larger or similar attenuation lengths to protons up to  $3 \times 10^{20}$  eV.

[1]. Similarly, heavy nuclei are broken up due to photo-disintegration. A compilation of energy loss lengths of protons and heavier nuclei is shown in Figure 1 [5]. Since the energy loss processes for protons and nuclei are different the evolution of composition during propagation has to be taken into account.

Alternative, non-acceleration scenarios for ultra-high energy cosmic rays have been proposed, such as the decays of topological defects or super-heavy dark matter. All of these models predict high fluxes of gamma rays and neutrinos. Finally there are propagation models in which the GZK energy loss processes are evaded or shifted to higher energies. Examples are violation of Lorentz invariance, the  $Z$ -burst model or postulation of new particles with properties similar to protons. Reviews of such alternative scenarios can be found in [8, 9]. They are now disfavoured except for the highest energies due to already stringent limits on the flux of photons.

Measurements of the arrival direction distribution, primary mass composition and energy spectra are the keys to solving the puzzle of ultra-high energy cosmic particles. High statistics is particularly important at the highest energies, where magnetic deflections are minimal and even charged particles are expected to point back to their source regions.

## 2 The Pierre Auger Observatory

The Pierre Auger Observatory for the highest-energy cosmic rays has been developed and built by more than 350 scientists in 17 countries. The southern site in Mendoza, Argentina, will be completed during the year 2008. The Observatory comprises 1600 water-Cherenkov detectors deployed over 3000 km<sup>2</sup> on a triangular grid with 1500 m spacing. This surface detector array (SD) is overlooked by 24 electronic telescopes, which are arranged in four stations around the SD area. The telescopes record images of the faint, ultra-violet fluorescence light excited by the air showers. The fluorescence detector (FD) operates on clear dark nights and achieves a duty cycle of 13 percent. The properties and performance of the prototype instruments have been published in 2004 [3]. A recent description of the combined hybrid operation of the SD and FD systems of the Auger Observatory can be found in the proceedings of the ICRC 2007 [4].

The layout and deployment status as of June 2008 is shown in Figure 2. The data set underlying the results reported here has been collected basically from January 2004 to August 2007. During this time the SD system grew from 154 to 1200 tanks and the FD system from 6 to 24 telescopes. The exposure over this period is three times greater than that of AGASA, similar to the monocular HiRes exposure, and corresponds to about 80 percent of a full Auger-year. Above 1 EeV the Auger Observatory has recorded more events than all previous efforts together. Due restrictions to periods of good data quality have been applied. We propose to use the unit Linsley as a measure of the total exposure of cosmic ray observatories,  $1Linsley = 1km^2syr$ . At the time of writing (June 2008) the total Auger exposure is 10,000L. The expected future annual increment is 7000 L.

From the beginning the Auger Observatory had been conceived as a hybrid system, in which the SD and FD components are completely integrated. The merits of the SD include stable operation with 100 percent duty cycle and a relatively straightforward determination of the effective area times solid angle (the aperture), whereas the energy measurement has to rely heavily on Monte Carlo simulations. Complementary, the FD offers optical

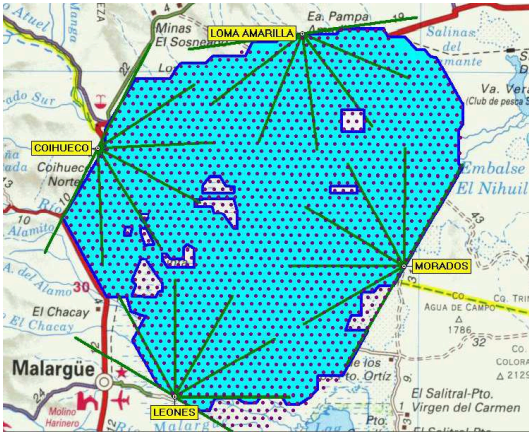


Figure 2: The southern Pierre Auger Observatory is located in the El Nihuel region in the Province of Mendoza, Argentina; the central campus is in the city of Malargüe. Dots indicate the 1600 surface detector positions. The four named fluorescence detector stations with six individual telescopes each are all operational, as well as the surface detectors within the shaded area.

shower detection in a calorimetric way and can be calibrated with very little dependence on shower models; however, the aperture grows with shower energy and its determination for all operating conditions is nontrivial.

A public internet display of 1% of the events recorded by the Auger Observatory is available online at <http://augersw1.physics.utah.edu/ED/>.

Each SD station is a 3.6 m diameter polyethylene tank containing a sealed liner with a reflective inner surface. The liner contains 12,000 l of pure water. Cherenkov light produced by the passage of particles through the water is collected by three nine-inch-diameter photomultiplier tubes, which are symmetrically distributed at a distance of 1.20 m from the center of the tank and look downwards through windows of clear polyethylene into the water. The surface detector station is autonomously operating with a 10 Watt solar power system. The electronics package includes a processor, GPS receiver, radio transceiver and power controller.

A vertically arriving cosmic ray shower of  $10^{19}$  eV typically triggers 8 detectors. SD signals are measured in units of a relativistic muon passing verti-

cally through the centre of a water-Cherenkov detector (vertical equivalent muon, VEM). This calibration of the SD array is performed continuously during data-taking with 2% accuracy. The number of secondary particles at observation level increases linearly with primary energy with some weak dependencies on the primary mass. The measured signal as a function of distance from the shower axis is fitted for individual events to obtain the VEM particle density at 1000m,  $S(1000)$ , which is used as an estimator of the size of each event. For energies above  $10^{19}$  eV, the relative uncertainty of  $S(1000)$  is about 10%, including contributions from counting statistics, from the imperfectly known lateral particle density distribution and from shower-to-shower fluctuations.

At least five active stations must surround the detector with the highest signal, and the reconstructed shower core must lie inside an active triangle of detectors. For most analyses we use showers up to zenith angles  $\theta < 60$  degrees. These quality cuts result in full acceptance above 3 EeV, and nearly constant exposure as function of  $\sin^2\theta$ . The effective area of the entire array at any time has been calculated from the number of active hexagons, which can be deduced from the low-level triggers sent by each detector every second. The integrated exposure is  $7000 \text{ km}^2 \text{ sr yr}$  and is known to 3%. Periods corresponding to less than 10% of the integrated exposure had data acquisition problems and were removed.

The angular resolution of the surface detector was determined experimentally, checked using the pairs data set and found to be better than  $2^\circ$  for 3-fold events ( $E < 4 \text{ EeV}$ ), better than  $1.2^\circ$  for 4-fold and 5-fold events ( $3 < E < 10 \text{ EeV}$ ) and better than  $0.9^\circ$  for higher multiplicity events, which have more than 10 EeV.

The FD measures the longitudinal development of cosmic ray showers in the atmosphere. Each individual telescope of the FD images a portion of the sky of 30 degrees in azimuth and elevation. Light is collected by a segmented spherical mirror of  $3.6 \times 3.6 \text{ m}^2$  through a UV-transparent filter window and a ring corrector lens to reduce the aberrations inherent in the Schmidt optics. The camera consists of 440 hexagonal photomultipliers, each with a field of view of 1.5 in diameter. The signals are continuously digitized at 10 Ms/s, temporarily buffered and searched for shower track patterns in real time.

The timing of FD and SD systems are synchronized to about 120 ns. The data are merged offline in the event building process.

The fluorescence light produced by the shower is detected as a line of pixels in the FD camera. The plane defined by the orientation of pixels, together with the timing information, is used to determine the shower direction. The pixel signal must be corrected for attenuation of the fluorescence light due to Rayleigh and aerosol scattering along its path toward the telescope, and for a contribution of direct and scattered Cherenkov light. The fluorescence light is then proportional to the electromagnetic energy deposited by the shower along its path in the atmosphere. The reconstructed energy profile is fitted with a Gaisser-Hillas function [2], which provides a measurement of the maximum depth of the shower, and of the shower energy. A final correction for missing energy due to high-energy muons and neutrinos amounts to about  $(10 \pm 4)\%$ . This procedure provides a nearly calorimetric, model-independent energy measurement with a resolution of 8%.

The absolute fluorescence yield of the 337 nm band in air is 5.05 photons/MeV of energy deposit at 293 K and 1013 hPa, derived from [10]. We use the measurements of [11] for the wavelength and pressure dependence of the fluorescence spectrum.

The absolute calibration of the FD telescopes is known to 10%. The relative response of all FD channels is determined twice every night illuminating the cameras from pulsed LEDs and/or Xe flashers. The absolute calibration is performed less frequently. In this case the whole aperture is illuminated by a flat-field source with known spectral and directional characteristics and known intensity, calibrated at the National Institute of Standards and Technology. Atmospheric monitoring is an integrated part of the FD operation. The system consists of four single wave-length LIDAR stations, one Raman LIDAR, several weather stations, balloon born meteorological probes, remote-controlled laser and dedicated aerosol monitors.

The systematic uncertainties in setting the FD energy scale sum to 22%. The largest uncertainties are due to the absolute fluorescence yield (14%), the absolute calibration of the FD (10%) and the reconstruction method (10%), while the influence of pressure, humidity and temperature, the wavelength dependent response of the FD, the

aerosol phase function, missing energy and others are smaller.

Instrumental enhancements are currently being installed close to the Coihueco FD station. These include underground muon detectors, additional water Cherenkov detectors, high-elevation fluorescence telescopes for a larger field-of-view and radio antenna to detect the geo-synchrotron emission of air showers.

### 3 The Energy Spectrum

Combining the SD and FD information, the energy can be estimated for each event by a method that relies almost entirely on data and depends very little on hadronic interaction models or assumptions about the nature of the primary particle. We use the so-called *constant intensity cut* method [12], by which the zenith angle dependence of  $S(1000)$  is derived from the assumption that the true cosmic ray intensity at a given energy should be the same for all directions. Using a suitably chosen reference intensity we normalize  $S(1000)$  for each event to the signal it would have had at a zenith angle of  $38^\circ$ , which is the median zenith angle of the events of interest. That quantity called  $S_{38}$  is used to correlate with the calorimetric energy measurement by the FD for currently 661 selected high-quality hybrid events. To avoid efficiency and selection biases, low energy events are discarded from the calibration sample. The fitted power law  $E_{FD} = 1.49 \times 10^{17} eV \times S_{38}^{1.08}$  indicates that  $S_{38}$  grows approximately linear with energy. The energy resolution estimated from the root mean square deviation of the distribution is 19%, which is in good agreement with the quadratic sum of the SD and FD energy uncertainties.

The energy spectrum based on 20,000 SD events with the energy scale set by the FD as described above is displayed in Figure 4. The total systematic energy scale uncertainty is 22% as described in the previous section. The residuals relative to a spectrum with a spectral index of 2.69 is also shown together with data from the HiRes experiment [25]. No data from the AGASA experiment are shown as they are currently under revision [24]. The Auger data show the flux suppression above  $4 \times 10^{19}$  eV with 6 standard deviations.

Statistics and energy range can be extended by

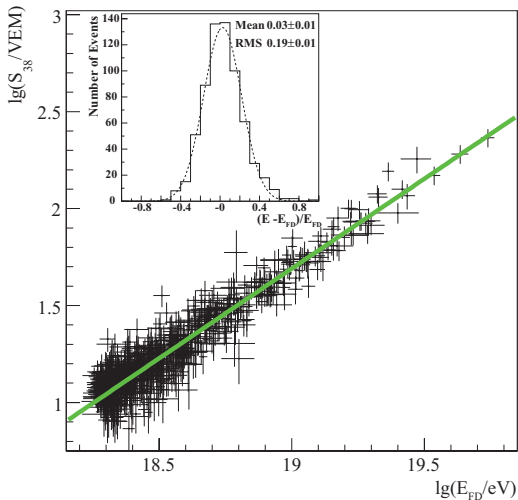


Figure 3: Correlation between surface detector signal and FD energy for 661 hybrid events used in the fit. The full line is the best fit to the data; the fractional differences between the two energy estimators are shown in the inset.

including inclined showers with zenith angles larger than  $60^\circ$  and hybrid events, which have at least one SD detector together with a FD track recorded. The inclined events add another 1,500 L to the data set at all energies; special reconstruction efforts are currently being devised for events with zenith angles larger than  $80^\circ$ , where the particle distributions are significantly distorted due to absorption in air and the Earth's magnetic field.

## 4 The Primary Mass Composition

Measuring the composition of cosmic rays is crucial in order to obtain a full understanding of their acceleration processes, propagation and relation with galactic particles. The atmospheric depth  $X_{max}$  denotes the longitudinal position of the shower maximum, which is directly accessible with the FD. It grows logarithmically with the energy of the primary particle. The behaviour of  $X_{max}$  for different primary particles like photons, protons and heavier nuclei can be conceptually understood in the framework of Heitler models [13], which are in good

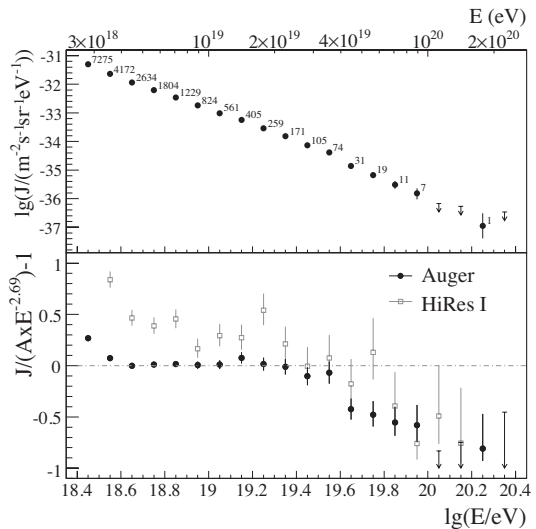


Figure 4: Upper panel: Differential flux as a function of energy. Vertical error bars represent the statistical uncertainty only. The number of events in each bin is also given. Lower panel: Fractional differences between Auger and HiRes I data relative to a spectrum with an index of 2.69.

agreement with detailed Monte Carlo simulations. Data and models for Auger hybrid events are shown in Figure 5. The apparent change from lighter to heavier particles above  $2 \times 10^{18}$  eV is an interesting feature, which is currently under investigation.

## 5 The Photon and Neutrino limits

Photon induced air showers would penetrate 200 - 300  $g/cm^2$  deeper into the atmosphere than protons. The observables sensitive to the longitudinal shower development are  $X_{max}$  measured with the FD, and the signal risetime and the curvature of the shower front measured in SD-only events. The first limit on the photon contents of cosmic rays at the highest energies had been derived from the fluorescence detector [14]; a more stringent result has now been derived using the large statistics of surface detector events. The maximum fraction of photons is 2.0% above  $10^{19}$  eV and 62% above  $8 \times 10^{19}$  eV, which corresponds to limits on the flux of photons

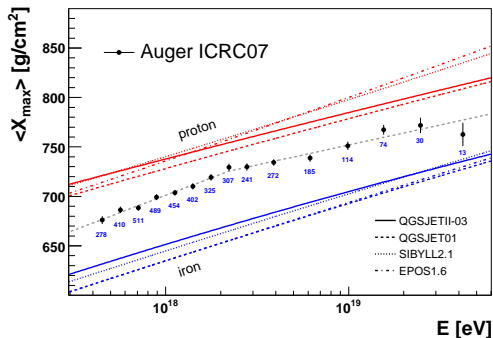


Figure 5: Atmospheric depth  $X_{max}$  of the shower maximum as a function of energy. The data points are accompanied by their respective number of events in each bin; the expectations for primary protons and iron nuclei are shown for three different models [23].

of  $6.9 \times 10^{-3}$  and  $1.7 \times 10^{-3} km^{-2} sr^{-1} yr^{-1}$ , respectively, with a confidence level of 95%. This new result [15] disfavors many exotic models of sources of cosmic rays as shown in Figure 6.

A large air shower array like Auger represents a significant target mass to high-energy astrophysical neutrinos. Neutrino induced showers can be identified if they occur deep in the atmosphere under large zenith angles, or by their special topology in the case of Earth-skimming tau neutrinos. Identification criteria have been developed to find EAS that are generated by tau neutrinos emerging from the Earth. No candidates have been found in the data collected between 1 January 2004 and 31 August 2007. We derive an upper limit on the diffuse tau neutrino flux as  $E_\nu^2 dN_\nu / dE_\nu < 1.3 \times 10^{-7} GeV cm^{-2} s^{-1} sr^{-1}$  in the energy range  $2 \times 10^{17} eV < E_\nu < 2 \times 10^{19} eV$ . In Figure 7 we show our result [16], which is at present the most sensitive bound on neutrinos in the EeV energy range. In the future, our sensitivity will improve by more than an order of magnitude.

## 6 The Arrival Directions

The search for anisotropies in the arrival directions of cosmic rays or even for distinct sources has been a long-standing goal. The Auger Col-

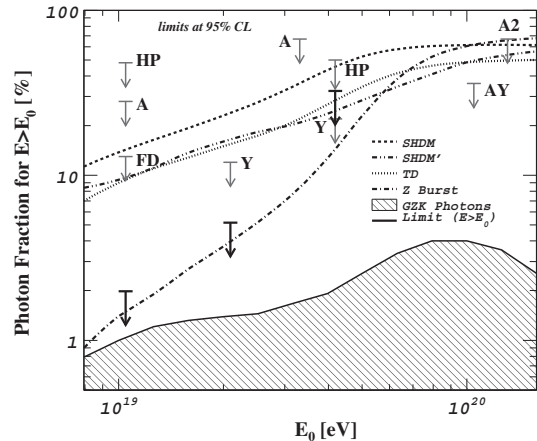


Figure 6: The upper limits on the fraction of photons in the integral cosmic-ray flux derived from SD events (black arrows) along with previous experimental limits (HP: Haverah Park; A1, A2: AGASA; AY: AGASA-Yakutsk; Y: Yakutsk; FD: Auger hybrid limit). Also shown are predictions from top-down models and for the GZK photon fraction. See [15] and references therein.

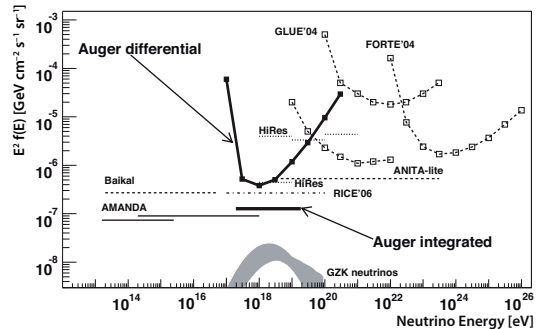


Figure 7: Limits at 90% C.L. for a diffuse flux of astrophysical neutrinos. Limits from other experiments are converted to a single flavour assuming a 1 : 1 : 1 ratio of the 3 neutrino flavours and scaled to 90% C.L. where needed. The shaded curve shows a typical range of expected fluxes of GZK neutrinos - predictions vary by an order of magnitude. See [16] and references therein.

laboration has recently published the observation of a correlation between the arrival directions of the most energetic cosmic rays and Active Galactic Nuclei (AGN) listed in the Veron-Cetty and Veron catalogue [17, 18]. An exploratory scan of an early data set had been performed in the parameter space given by the angular deviation between arrival directions and AGN positions, AGN distance (given by their redshift) and cosmic ray energies. Parameters were then fixed *a priori* and applied to an independent second data sample in order to avoid the complications and statistical penalties inherently present in *a posteriori* searches. The correlation has its maximum significance for energies greater than 57 EeV, AGN closer than about 71 Mpc distance and angular deviations within  $3.1^\circ$ . In this conference contribution a different representation in equatorial coordinates instead of galactic coordinates is shown in Figure 8.

This result has to be considered together with the flux suppression described previously; it is consistent with the hypothesis that the rapid decrease of flux measured by the Pierre Auger Observatory above 60 EeV is due to the GZK effect and that most of the cosmic rays reaching Earth in that energy range are protons from nearby extragalactic sources, either AGN or other objects with a similar spatial distribution. The maximum acceleration power of cosmic ray sources cannot be determined yet, but this alone cannot explain the sudden onset of the position correlation.

A rich spectrum of interesting science questions opens up when future observations of all sources on the sky with high statistics can be combined with detailed investigations of the primary particles' nature and their interactions at center-of-mass energies up to 350 TeV.

The Auger Collaboration has also searched for signals from the galactic center [19], and for clustering on different angular scales at the highest energies and for correlations with BL Lac objects. These studies [20, 21, 22] have not confirmed previous claims.

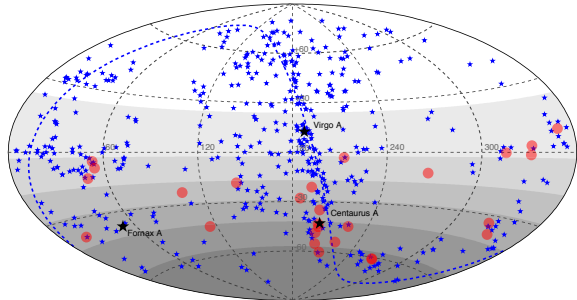


Figure 8: Map of the celestial sphere in equatorial coordinates. Colored circles with radius 3.1 degrees are centered at the arrival directions of the 27 cosmic rays with highest energy detected by the Pierre Auger Observatory. The positions of the 472 AGN with redshift  $z$  less than 0.018 (corresponding to distances up to 75 Mpc) from the 12th edition of the catalog of quasars and active nuclei by Veron-Cetty and Veron are indicated by the blue stars. Grey shading indicates larger relative exposure, which is maximum at the South celestial pole. Centaurus A, Fornax A, and Virgo A, three of the closest candidate sources, are marked with black stars. The super-galactic plane is shown as a dashed blue line.

## 7 The Northern Pierre Auger Observatory

The scientific challenge is to follow-up the recent results by the identification of sources over the whole sky and by the detailed study of the physical processes at work in such extreme conditions. These involve strong gravitational fields, high temperatures and densities, large magnetic and background radiation fields, and very high energies interactions. Multiple events from the most intense sources will allow a detailed study of the source characteristics and acceleration processes, while particle collisions at center of mass energies in excess of 300 TeV may reveal new insights to particle physics. Such measurements at Auger South have yielded unexpected results when compared with current interaction models. High statistics at the highest energies is essential to address these scientific objectives effectively. The Northern Auger Observatory (Auger North) will focus on achieving higher statistics at energies above  $6 \times 10^{19}$  eV, where the Greisen-

Zatsepin-Kuzmin effect makes it possible to study nearby sources without the isotropic background from the rest of the far universe.

Auger North will be built with a combination of the same basic elements as used in Auger South: surface particle detector stations, fluorescence telescopes, and an associated communications and calibration infrastructure. The site, chosen in 2005, is located in the South-East corner of the State of Colorado (USA), centered at about  $38^\circ$  N Lat,  $102^\circ 30'$  W Long. The average altitude is about 1300 m above sea level. The landscape is almost flat, gently rolling and open; it offers an exceptionally large area of more than 8,000 square miles (20,000 square kilometers), possibly spanning into the State of Kansas. An important feature is the system of county roads, which are spaced on a rectangular one-mile grid covering a large fraction of the anticipated deployment area.

The conceptual design includes a base grid of 4,000 SD stations to be positioned on every second corner of the square-mile grid, alternating in adjacent lines. The total area is 8,000 miles<sup>2</sup> or 20,000 km<sup>2</sup> with a detector spacing of approximately  $\sqrt{2} \times 1$  mile (2.3 km). Simulations suggest that this configuration reaches 50% efficiency at  $10^{19}$  eV and 100% efficiency at  $10^{19.5}$  eV. An embedded denser grid of 400 additional SD stations would be placed on the empty positions in 10 percent of the base grid in order to achieve full efficiency already at  $10^{19}$  eV for a subset of the events. The landscape requires a peer-to-peer data communication rather than a direct transmission from SD stations to centralized receivers. Almost full coverage of the SD system can be achieved with 40 to 50 fluorescence telescopes anticipating a maximum viewing distance of 40 kilometers.

Research and development works in order to improve performance and reduce cost have started some time ago and activities on the Northern site in South-East Colorado are ramping up. Technically, the construction of Auger North could begin in 2010. Figure 9 shows the exposures of current and future cosmic ray observatories as a function of time.

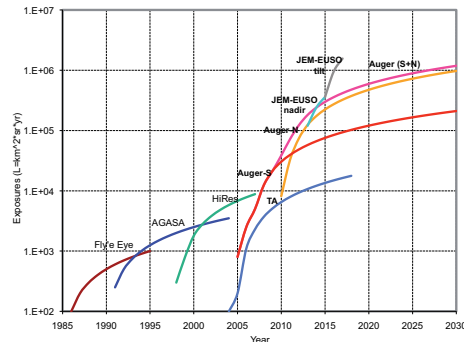


Figure 9: Exposures of cosmic ray observatories as a function of time. The JEM-EUSO project is a space-born instrument on the ISS, whereas the other installations are ground-based. [26].

## 8 Conclusion and outlook

The Pierre Auger Observatory has been collecting data of unprecedented quality since January 2004. First results include a measurement of the energy spectrum, which exhibits a flux suppression above 40 EeV as predicted by Greisen, Zatsepin and Kuzmin. The arrival directions of the most energetic cosmic particles are anisotropic and show a correlation with the positions of nearby extragalactic objects. Other previous claims of anisotropies or distinct sources have not been confirmed. Preliminary indications of the cosmic ray mass composition give rise to interesting interpretations. Based on the wealth of current data, a conceptual design for the Northern Auger Observatory has been presented.

## 9 Acknowledgement

I would like to thank the organizers of the *International Workshop on Advances in Cosmic Ray Science* held in March 2008 at Waseda University, Shinjuku, Tokyo, Japan; it was a pleasure taking part in the interesting presentations and discussions. I enjoyed the help of my Auger colleagues in the preparation of this report. I acknowledge the support from Forschungszentrum Karlsruhe, member of the Helmholtz Association of German Research Centers, and from the University of Karl-



sruhe, now joining forces in the *Karlsruhe Institute of Technology* KIT.

## References

- [1] K. Greisen, Phys. Rev. Lett. 16 (1966) 748; G. T. Zatsepin and V. A. Kuzmin, Pisma Zh. Eksp. Teor. Fiz. 4 (1966) 114.
- [2] T.K. Gaisser and A.M. Hillas, Proc. 15th ICRC, Vol. 8 (1977) p.353.
- [3] J. Abraham et al. [Pierre Auger Collaboration], Nuclear Instruments and Methods **A523** (2004), 50.
- [4] B. Dawson for the Pierre Auger Collaboration: 2007, Proc. 30th ICRC (Merida), no. 976 [arXiv:0706.3236v1].
- [5] D. Allard et al., JCAP 0609 (2006) 005 and astro-ph/0605327.
- [6] A. M. Hillas, Ann. Rev. Astron. Astrophys. 22 (1984) 425.
- [7] D. F. Torres and L. A. Anchordoqui, Rept. Prog. Phys. 67 (2004) 16631730 and astro-ph/0402371.
- [8] A. Bhattacharjee and G. Sigl, Phys. Rep. 327 (2000) 109.
- [9] M. Kachelriess, Comptes Rendus Physique 5 (2004) 441452 and hep-ph/ 0406174.
- [10] M. Nagano, K. Kobayakawa, N. Sakaki, K. Ando, Astropart. Phys. 22 (2004) 235.
- [11] AIRFLY Collaboration, M. Ave et al., Astropart. Phys. 28 (2007), 41.
- [12] J. Hersil et al. Phys. Rev. Lett. 6 (1961) 22.
- [13] J. Matthews, Astroparticle Physics 22 (2005) 387.
- [14] J. Abraham et al., [Pierre Auger Collaboration], Astroparticle Physics 27 (2007), 155.
- [15] J. Abraham et al., [Pierre Auger Collaboration], Astroparticle Physics 29 (2008), 243.
- [16] J. Abraham et al. [Pierre Auger Collaboration], Physical Review Letters 100 (2008), 211101.
- [17] J. Abraham et al. [Pierre Auger Collaboration], Science 318 (2007), 939.
- [18] J. Abraham et al. [Pierre Auger Collaboration], Astroparticle Physics 29 (2008), 188.
- [19] J. Abraham et al. [Pierre Auger Collaboration], Astroparticle Physics 27 (2007), 244.
- [20] E. Armengaud for the Pierre Auger Collaboration: 2007, Proc. 30th ICRC (Merida), no. 76 [arXiv:0706.2640v1]
- [21] D. Harari for the Pierre Auger Collaboration: 2007, Proc. 30th ICRC (Merida), no. 75 [arXiv:0706.1715v1]
- [22] S. Mollerach for the Pierre Auger Collaboration: 2007, Proc. 30th ICRC (Merida), no. 594 [arXiv:0706.1749v1]
- [23] M. Unger for the Pierre Auger Collaboration: 2007, Proc. 30th ICRC (Merida), no. 594 [arXiv:0706.1495v1]
- [24] M. Teshima, Int. Conf. on Astroparticle Physics, Rome 2007.
- [25] R.U. Abbasi et al., Phys. Rev. Lett. 100 (2008) 101101.
- [26] A. Olinto, Symmetry Phases Symposium, Irsee, Germany (2008).